Metal-Insulator-Metal Gas Sensor Based on Polarizable Thin Films

Martin Schreivogel, Denis Kunz,
Ralf-Roman Rosenberger
Corporate Research
Robert Bosch GmbH
Stuttgart, Germany
martin.schreivogel@de.bosch.com

Martin Schreivogel, Wolfgang Menesklou, Ellen Ivers-Tiffée
Institute of Materials for Electrical and Electronic Engineering
Karlsruher Institut für Technologie (KIT)
Karlsruhe, Germany

Abstract— **A new type of Metal-Insulator-Metal (MIM) gas sensor sensitive to low concentrations of hydrogen containing gases is presented. Less than 5 ppm H_2 give rise to significant signal changes compared to pure nitrogen or air. Response times are in the order of several ten seconds. The capacitive structure incorporates two stacked dielectric thin films (SiO_2, Al_2O_3) with a thickness of a few ten nanometers sandwiched between platinum electrodes. The oxides show a distinct polarization mechanism that influences the dielectric properties of the films at elevated temperatures above 200 °C. The devices are characterized by *I-V* measurements and impedance spectroscopy. The mobile species create an additional polarization mechanism that can be influenced by an appropriate DC bias. At low biases the dipoles are moveable in the oxide, so they can change their direction by an applied alternating field. At high biases the dipoles are pinned in one direction and the impedance spectrum of the device corresponds to an almost ideal capacitor with no loss mechanisms. Similar to an externally applied DC bias, species from the gas phase that are adsorbed at the electrode-insulator interface can introduce an electric field in the dielectric thin film influencing the mobility of the species. Thus, the contribution of the polarization mechanism to the impedance depends on the gas atmosphere and the change of its real or imaginary part can be used as sensor signal. Additionally, with this new gas sensor structure one can achieve selectivity for reducing and oxidizing gases by choosing appropriate operating points set by a DC bias.**

Keywords-gas sensor; hydrogen; silicon dioxid; aluminum oxid; polarization; impedance spectroscopy

I. INTRODUCTION

Gas sensors play a major role in monitoring and controlling many kinds of technological processes. One prominent example is the use of hydrogen as a renewable energy carrier for automotive or stationary fuel cell applications. Although there are many optimistic predictions concerning hydrogen based technologies, safety issues remain a critical aspect for hydrogen storage and transport [1]. Therefore, sensing hydrogen leakage with very high sensitivity is essential for the introduction of hydrogen as fuel for commercial applications.

During the last decade different physical mechanisms for the detection of hydrogen have been investigated. To name but a few, there are sensors that use hydrogen partial pressure sensitive optical constants, temperature changes due to different heat conductivities, resistivity changes of metal oxides and field effect devices that detect adsorbed gas species on their catalytically active gate electrode [2-6]. Most of these approaches involve quite elaborate preparation techniques and many different process steps. Furthermore, relatively complex devices still face considerable challenges concerning their long term stability.

We report a new kind of highly sensitive hydrogen gas sensor incorporating a polarizable thin film. The design of the sensor is extremely simple as it is basically a parallel plate capacitor.

At first appearance, one would not expect such a dielectric capacitance with a dense electrode to be gas sensitive. Therefore, after presenting the structure itself and its gas sensitivity in subsection II.A we performed current-voltage measurements (II.B) and impedance spectroscopy (II.C) in order to understand the physical mechanisms. Based on these measurements we propose a first model for the signal mechanism and an equivalent circuit in section II.C and II.D. Finally, we emphasize the potential of the MIM structures for selective gas detection in subsection II.E.

II. EXPERIMENTAL RESULTS AND DISCUSSION

A. *Investigated structure and gas sensitivity*

Fig. 1 depicts a schematic drawing and scanning transmission electron micrograph (STEM) of the examined metal-insulator-metal (MIM) structure. The two dielectric layers are sandwiched between two dense platinum electrodes. Plasma-enhanced chemical vapor deposited (PECVD) SiO_2 was chosen to promote the adhesion of the following atomic layer deposited (ALD) Al_2O_3. Aluminum oxide is known to show good stability when exposed to gas at elevated temperatures from our former studies [7]. There was no additional annealing step after deposition and the microstructure of the oxide films is amorphous whereas the platinum is polycrystalline, which was shown by the STEM measurements. The layout of the different layers was designed in a way that dielectric breakthroughs are avoided.

In a first step, the effective capacitance (calculated from the measured impedance with the assumption of an RC element as equivalent circuit for the structure) of the MIM structures was measured at a fixed frequency when they were exposed to different gases. The response to different

ISBN: 978-1-61208-297-4

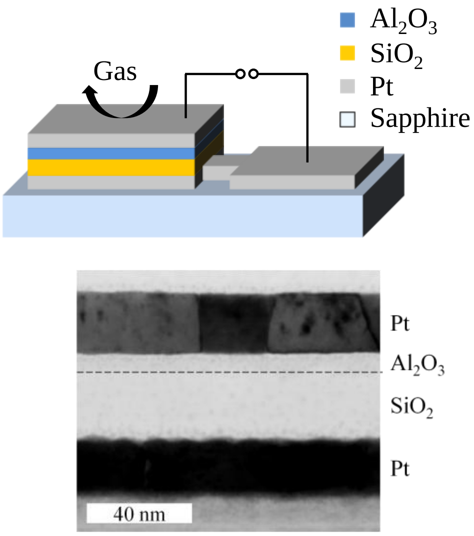

Figure 1. Schematic drawing and STEM micrograph of the examined MIM structure. They consist of a stack of a platinum back contact (20 nm), silicon oxide (23 nm), aluminum oxide (6 nm) and a dense platinum front electrode stacked on a sapphire substrate (to enhance the contrast between SiO_2 and Al_2O_3 a dashed line was added).

concentrations of hydrogen is shown in Fig. 2. The reference gas was pure nitrogen. The devices show a very high sensitivity and presumably it is possible to measure much lower concentrations, because the small signal change between 5 and 20 ppm suggests that the response is already close to saturation in this range (our home designed measurement system is limited to a minimum concentration of 5 ppm).

There was no response observed, when the device was exposed to NO or NO_2. However, there is cross-sensitivity towards other hydrogen-containing gases like C_2H_6 or NH_3.

As mentioned earlier, these clear and steplike hydrogen signals are surprising for a structure like this which incorporates none of the known transducer mechanism usually utilized for gas sensing. Since geometric changes of the dielectric layers can be ruled out as the origin of the capacitance change there has to be a variation of the electric properties of the dielectric thin films due to different gas atmospheres.

To explain these effects and to understand the most interesting gas sensitivity we systematically performed further electrical characterizations that are presented in the following subsections.

B. *I-V measurements*

One approach to explain the gas sensitivity is an influence of the hydrogen on the electronic or protonic DC conductivity of the dielectric films. Zhu et al. observed a hydrogen-induced increase in the direct current through an amorphous $(Ba_{0.67}Sr_{0.33})Ti_{1.02}O_3$ (BST) MIM structure when it was exposed to hydrogen. They explained it by an induced polarization potential at the electrode-BST interface [8]. To compare their results and validate their theory for our structures we measured the current through the dielectric as function of voltage in pure nitrogen and 100 ppm hydrogen (see Fig. 3). In order to gain information about non-steady state processes we introduced a delay between voltage application and current measurement at each point. By increasing the delay the scan rate was decreased and consequently there was more time for the relaxation of non-steady state processes such as polarization currents. The temperature was set to 350 °C, only at these elevated temperatures the below described effects emerge.

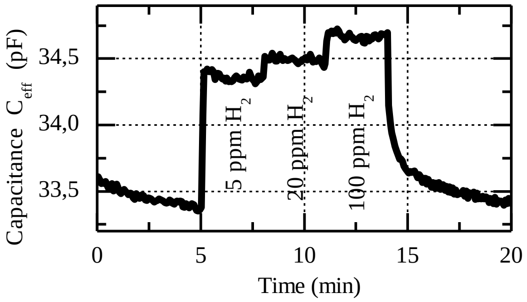

Figure 2. Response of the MIM structure to 5, 20 and 100 ppm hydrogen in nitrogen. The measurement frequency was 100 Hz and the device temperature was set to 350 °C.

In all the measurements there are distinct current maxima observed. They occur at voltages that are supposed to correspond to the flat band condition in the dielectric layers, that means at these biases the electric field in the dielectrics becomes zero. They occur in both scan directions showing some hysteresis. In nitrogen these maxima are not arranged symmetrically to zero volts. Possible reasons for this could be different work functions of the metal electrodes or fixed charges trapped in one of the oxides.

When the delay between voltage application and current measurement is increased, i.e., the scan rate is decreased, the described maxima vanish. This behavior indicates that there is a contribution to the current that is no continuous leakage current but some kind of polarization current. It should be noticed that the according polarization mechanism arises from the dielectric film itself and can’t be explained by the charging of the geometrical capacitance as the time constant is at the order of several seconds.

Another observation that can be made in the current-voltage measurements concerns the effect of hydrogen. At the same scan rate the whole curve seems to be shifted towards lower voltages when exposed to 100 ppm hydrogen. Thus, the hydrogen acts like a voltage offset at the electrode. This offset can be understood as work function change of the platinum at the platinum-dielectric interface induced by adsorbed hydrogen [9]. From literature it is well known that hydrogen is able to diffuse through platinum thin films [10]. This is not the case for gases like NO or NO_2, which explains the observed selectivity towards hydrogen-containing gases for structures with dense front electrodes.

From the *I-V* measurements it can be concluded that the mechanism described by Zhu et al. is not the origin for the gas sensitivity of our structures. However, we got some first

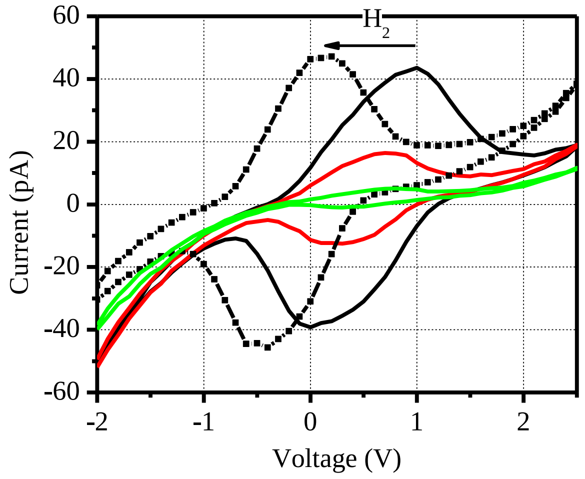

Figure 3. I-V-curves measured on the MIM structures in different gas atmospheres and with different scan rates. The step size of the scan was 100 mV and there was a delay between voltage application and current measurement at each point. The delay was 5 s, 15 s and 60 s (black, red, and green, respectively) for the curves in nitrogen at the right and 5 s for the curve in 100 ppm hydrogen in nitrogen at the left (square symbols).

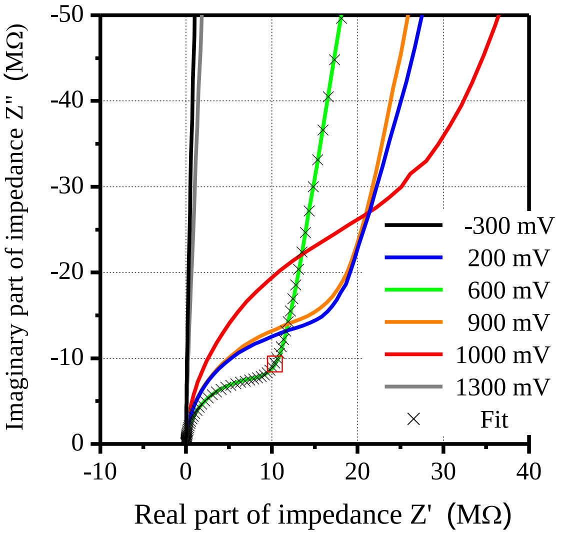

Figure 4. Impedance spectra of the MIM structures at different biases. The measurements were carried out at frequencies from 1 MHz down to 100 mHz (for clarity reasons there is only 1 MHz to 10 Hz depicted; the small red square marks the measured data at 100 Hz.) and at a temperature of 350 °C. The black crosses are fit values corresponding to the equivalent circuit model discussed in subsection D.

ideas of the signal formation mechanism for which an additional polarization mechanism seems to play a major role. Thereby motivated, we performed impedance measurements that are a common technique to characterize dielectric thin films with polarization losses.

C. *Impedance measurements*

In order to gain more information about the nature of the present polarization mechanism we measured the impedance of the structures as a function of frequency. To interpret these impedance spectroscopy data we chose Cole-Cole diagrams, which show the imaginary part Z'' of the impedance as a function of the real part Z', where $Z=Z'+jZ''$. Fig. 4 shows the spectra for different biases applied to the capacitances. In a certain bias range there is clearly an additional polarization mechanism present. It is expressed by the semicircle emerging for small impedances having a minimal radius at a bias of approximately 600 mV. This is in good agreement with the offset of the centre of the *I-V* curves from zero described in subsection B. For biases that are more than about 500 mV away from that value the Cole-Cole plot of the impedance spectrum shows almost a vertical line, which corresponds to an ideal capacitor with small losses. That means the impedance consists basically of a frequency-dependent imaginary part $Z''=-(\omega C)^{-1}$, where ω is the angular frequency and C the capacitance. This implies that there are polarizable species that are free to move when there is no net electric field in the dielectrics. Under these circumstances they contribute significantly to the impedance of the structure with a time constant at the order of 10 s. On the other hand the dipoles are pinned at one side or in one orientation when the magnitude of the applied voltages is relatively high.

The actual microscopic origin of the observed polarization and the relative contribution of the different oxides are subject of current investigations. There are different mechanisms like drifting ionic impurities or the switching of monovalent impurity ions, that are connected to the amorphous structure by non-bridging oxygen ions, imaginable [11]. In both cases the ongoing processes are thermally activated, which explains the need of temperatures above approx. 200 °C to observe the described effects.

The reason for the gas sensitivity of the structures can be examined with impedance measurements as well (see Fig. 5). The adsorbed hydrogen affects the whole frequency range and has the same effect as an additional bias of about 400 to 600 mV (compare to the bias-dependent measurements in nitrogen atmosphere in Fig. 4). This effect is at the same order of magnitude as the shift of the *I-V* curves in Fig. 3.

Additionally, from Fig. 5 the measured gas signal at one specific frequency can be understood in detail. As an effect of the adsorbed gas accompanied by the induced bias offset the influence of the polarization mechanism on the impedance spectra changes. This in general means that both the real and imaginary part of the measured impedance change. From this point of view the first way of plotting the gas signal in Fig. 2 as effective capacitance might be confusing because the assumption of an ideal capacitor for the calculation of the capacitance C_{eff} is invalid. To describe a system like this a little more complex equivalent circuit is necessary. A first suggestion is given in subsection D.

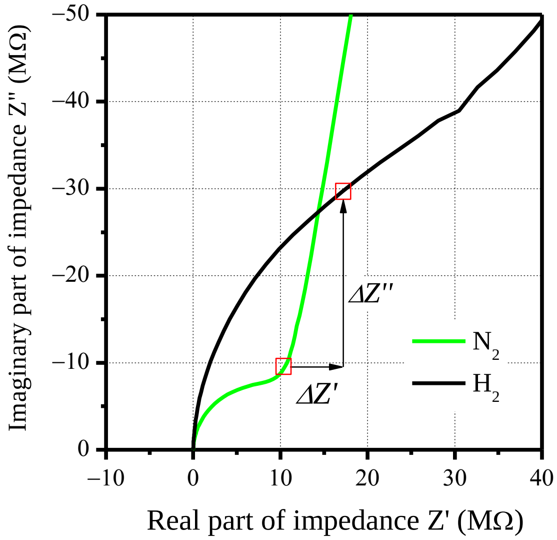

Figure 5. Impedance spectra of the MIM structures in pure nitrogen and 100 ppm hydrogen in nitrogen. In both cases the DC bias was 600 mV and the temperature 350 °C. The small red squares mark the measured data at 100 Hz.

D. *Proposed equivalent circuit*

In order to quantitatively describe the behavior of the MIM structure it is desirable to use an equivalent circuit model. As a first step we propose the circuit shown in Fig. 6. An impedance spectroscopy specialist might realize that the same electrical behavior can be described by a series connection of two RC elements. Nevertheless, we think that the shown approach is the physically more intuitive one. The physical meanings of the four components are as follows:

C_{geo} is the geometrical capacitance of the structure. Its origin is the charging of the parallel plate capacitor taking into account the bias-independent permittivity of the dielectrics at high frequencies:

$$C_{geo} = \varepsilon_0 \varepsilon_{r,eff}^{hf} \frac{A}{d} = \varepsilon_0 \frac{\varepsilon_{r,1}^{hf} \varepsilon_{r,2}^{hf}}{\varepsilon_{r,1}^{hf} d_2 + \varepsilon_{r,2}^{hf} d_1} A, \qquad (1)$$

where ε_0 is the permittivity of vacuum, $\varepsilon_{r,eff}^{hf}$ is the effective relative permittivity of the dielectric stack at high frequencies, $\varepsilon_{r,x}^{hf}$ and d_x are the relative permittivity and thickness of layer x, with $d=d_1+d_2$ and A is the area of the capacitor. C_{geo} is assumed to be constant for all applied biases and frequencies.

R_{el} is the resistance towards electronic leakage currents through the dielectric materials. It should be noted that in general R_{el} is not ohmic but depends on the applied voltage as there are different electronic conduction mechanisms like Schottky thermoionic emission or Poole-Frenkel conduction imaginable [12].

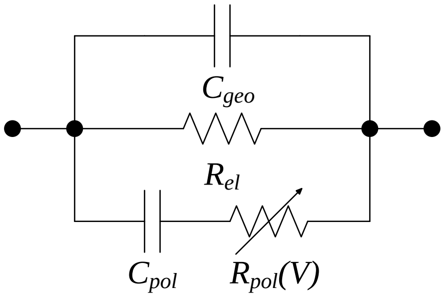

Figure 6. Equivalent circuit model for the MIM structure at elevated temperatures. C_{geo} is the geometrical capacitance, R_{el} the electronic leakage current and C_{pol} and R_{pol} represent the influence of the additional polarization mechanism.

The lower branch of the circuit is intended to describe the additional low frequency gas- and bias-dependent polarization mechanism for biases close to zero. Obviously there has to be an additional capacitance C_{pol} as the polarization allows a higher charge to be stored on the MIM structure at a certain voltage. To improve the agreement of the measured and fitted data one practically uses a so called constant phase element (CPE) instead of an ideal capacitance. The impedance of an CPE includes a correction coefficient n to describe deviations from ideal capacitances like rough electrode surfaces: $Z_{CPE}=((i\omega)^n C_0)^{-1}$ [13].

R_{pol} is implemented to take the polarization losses into account. Furthermore the series connection of C_{pol} and R_{pol} means that there is no continuous current through the lower branch of the parallel circuit. This physically makes sense since the species that are polarized are restricted to the dielectric layers and it is a consequence of the observations in Fig. 3.

In order to describe the observed bias dependence of the polarization, R_{pol} is not a constant, but changes with the bias, which can be seen by the varying diameter of the first semicircle. That means, an increased R_{pol} describes the reduced mobility of the dipoles in high electric fields and it shows a minimum at around 600 mV in nitrogen.

The presented model exemplary was fitted to the curve measured with a bias of 600 mV in Fig. 4. The extracted parameters are listed in Table 1. They all lie in the expected order of magnitude. For example C_{geo} with (1) can be estimated to be approximately (39±8) pF, using reasonable errors for the geometric dimensions (5%) and for the permittivities $\varepsilon_{r,SiO2}^{hf}$ =4.0±0.5 and $\varepsilon_{r,Al2O3}^{hf}$ =7.0±1.0 [14].

TABLE 1. FIT VALUES FOR THE EQUIVALENT CIRCUIT MODEL IN FIG. 6 AND THE IMPEDANCE DATA SHOWN IN FIG. 4 (600 MV)

C_{geo}	R_{el}	$C_{pol,0}$	n	R_{pol}
(33.7±0.5) pF	(13.4±0.4) GΩ	(398±3) pF	0.894±0.2	(13.6±0.1) MΩ

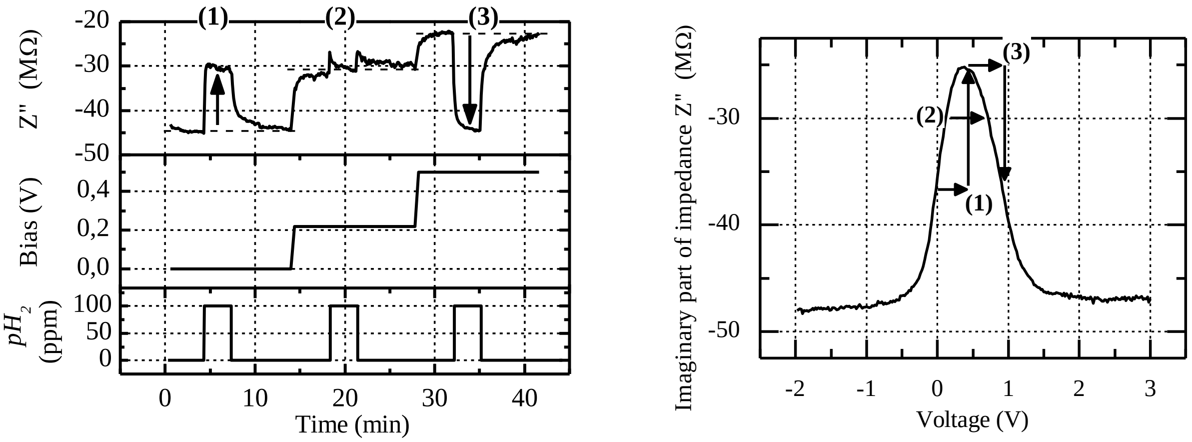

Figure 7. Gas signal - i.e. change in the imaginary part of the impedance - of the MIM structure for 100 ppm H_2 in nitrogen at different biases (left). The different polarities of the signal for different biases can be explained qualitatively by considering the dependence of the imaginary part of the impedance on the bias (right), showing a distinct peak. The horizontal arrows represent a constant voltage offset induced by the hydrogen starting from the externally applied bias.

E. Potential for selective gas measurements

Since it was observed that there is a relatively narrow bias range within which the described polarization mechanism occurs, the operating point, i.e., DC bias, at which the gas measurement is accomplished, obviously plays a critical role. This phenomenon is shown in Fig. 7. Here the imaginary part of the impedance was chosen as signal variable, the real part or the magnitude could be reasonable as well. According to which bias is chosen the gas signal can change its polarity or be completely suppressed. This behavior can be understood by considering the dependence of the impedance on the bias. There is a distinct peak of *Z''* at a bias that is supposed to represent flat band condition in the dielectric, which means maximal mobility of the polarizable species. According to which bias is chosen an additional voltage offset caused by the adsorption of hydrogen will lead to an increasing or decreasing impedance and in one special case to no signal at all. It also can be concluded that there is going to be no gas signal for voltages smaller than minus one or bigger than plus two volts.

The described dependence of the working point implies great potential for selectivity of the sensor towards different gases. For example gases that induce a positive voltage offset like hydrogen will lead to a maximal positive gas signal for operating points somewhat below the position of the peak of the impedance.

Inversely, gases that cause negative voltage offsets will lead to maximal signal when the operating point is above the position of the mentioned peak. Of course, it will be necessary to employ porous electrodes to enable the adsorption at the electrode-dielectric interface for other gases than hydrogen.

III. CONCLUSIONS

A new kind of gas sensor that stands out by a very elementary structure, simple fabrication, robustness, and high sensitivity is presented. By choosing the proper operating point impedance signal changes of almost 100 % for 100 ppm hydrogen can be realized. We propose a first equivalent circuit model and are able to explain the observed gas sensitivity with the acquired knowledge of the system. On this basis it is possible to predict a gas-selective operation mode of the device. The calibration of the sensors, the gas selectivity, the long-term stability and the microstructural investigation of the observed polarization mechanism will be subject of our further work.

ACKNOWLEDGMENTS

We would like to thank MicroGaN GmbH for the processing of the samples and the German Federal Ministry of Education and Research for financial support of the publicity sponsored project “InoSens”.

REFERENCES

[1] Y.-H. Chen, C.-Y. Chen, and S.-C. Lee. „Technology forecasting of new clean energy: The example of hydrogen energy and fuel cell,” African Journal of Business Management, vol. 4, 2010, pp. 1372–1380.

[2] P. Tobiška, O. Hugon, A. Trouillet, and H. Gagnaire, “An integrated optic hydrogen sensor based on spr on palladium,” Sensors and Actuators B: Chemical, vol. 74, 2001, pp. 168 – 172.

[3] I. Simon and M. Arndt, “Thermal and gas-sensing properties of a micromachined thermal conductivity sensor for the detection of hydrogen in automotive applications,” Sensors and Actuators A: Physical, vol. 97–98, 2002, pp. 104 – 108.

[4] O. K. Varghese, G. K. Mor, C. A. Grimes, M. Paulose, and N. Mukherjeeb, “A titania nanotube-array room-temperature sensor for selective detection of hydrogen at low concentrations,” Journal of Nanoscience and Nanotechnology, vol. 4, 2004, pp. 733–737.

[5] K. I. Lundström, M. S. Shivaraman, and C. M. Svensson, “A hydrogen-sensitive pd-gate mos transistor,” Journal of Applied Physics, vol. 46, 1975, pp. 3876–3881.

[6] J. Schalwig, P. Kreisl, S. Ahlers, and G. Muller, “Response mechanism of sic-based mos field-effect gas sensors,” Sensors Journal, IEEE, vol. 2, 2002, pp. 394 – 402.

[7] D. Kunz, R. Fix, and A. Martin, “Detection device for detecting gas within operating temperature range of detection device, has electrically conductive metal electrode and rear electrode made of metal or semiconductor material,” Patent DE-102009029621 A1, 2009.

[8] W. Zhu, O. K. Tan, and X. Yao, “Amorphous ferroelectric $(Ba_{0.67}Sr_{0.33})Ti_{1.02}O_3$ thin films with enhanced H_2 induced interfacial polarization potential,” Journal of Applied Physics, vol. 84, 1998, pp. 5134–5139.

[9] M. Fleischer and M. Lehmann, Solid State Gas Sensors - Industrial Application. Springer series on chemical sensors and biosensors, Springer, 2012.

[10] I. Lundström, H. Sundgren, F. Winquist, M. Eriksson, C. Krantz-Rülcker, and A. Lloyd-Spetz, “Twenty-five years of field effect gas sensor research in Linköping,” Sensors and Actuators B: Chemical, vol. 121, 2007, pp. 247 – 262.

[11] F. Argall and A.K. Jonscher, “Dielectric properties of thin films of aluminium oxide and silicon oxide,” Thin Solid Films, vol. 2, 1998, pp. 185 – 210.

[12] K. C. Kao, Dielectric Phenomena in Solids - With Emphasis on Physical Concepts of Electronic Processes, Elsevier Academic Press, 2004.

[13] J. R. Macdonald, E. Barsoukov (Editor), Impedance Spectroscopy: Theory, Experiment, and Applications, 2nd Edition, Wiley, 2005.

[14] S. Jakschik, U. Schroeder, T. Hecht, M. Gutsche, H. Seidl, and J. W. Bartha, „Crystallization behavior of thin ALD-Al_2O_3 films,” Thin Solid Films, vol. 425, 2003, pp. 216 – 220.

ISBN: 978-1-61208-297-4